# Application of Virtual Reality Technology in the Design of Interactive Interfaces for Public Service Announcements

Rong Hu
College of Visual Arts, Hunan Mass Media Vocational and Technical College, Changsha, 410100, China

***Abstract*—With the development of technology, more and more public service announcements are being designed with interactive interfaces. There are many different ways to interact with interactive interfaces, and using appropriate design methods can expand the impact of PSAs. The study incorporates image pre-processing methods based on virtual reality, using the cvtColor grey scale function and median filtering method to process the images, an iterative approach to camera positioning method design, and subsequent performance testing of the research algorithms. The test results showed that the peak signal-to-noise ratio of the research method was 13.390dB in the image pre-processing process and 35.635dB on lightly shaded images; in the error test, the rotational mean error of the research method was approximately 4.2degrees at four reference points; and in the image plane reprojection test, 70% of the points of the research method almost coincided with the original point position. The method generated 1203 designs with 40 reference points. The experimental results show that the research method can effectively design interactive interfaces for PSAs in virtual reality environments, and can propose more design solutions, and has better performance in virtual reality environment positioning.**

***Keywords*—*Virtual reality; interactive interfaces; interface design; greyscaling; image pre-processing***

## I. Introduction

With the increasing abundance of entertainment content on the Internet, people's acceptance of advertising is becoming lower, which puts forward higher requirements for the dissemination form of public service advertising [1]. Public service advertising has a certain degree of specificity, and traditional advertising forms and communication methods lack interaction with the audience, often making it difficult to achieve the expected promotional effect [2]. At present, the purpose of public service advertising is not only to disseminate information, but more importantly, to awaken the public's sense of social responsibility and promote social civilization and progress [3]. How to design public service advertisements that can stimulate public emotions and increase participation has become an urgent problem to be solved. At present, common interactive design methods for public service advertisements include socialized interaction, emotional guidance, etc. However, due to the limitations of communication carriers and audience groups, the design effect of public service advertisements is not ideal. With the continuous development of virtual reality technology, its application in various fields is becoming increasingly widespread. Virtual reality technology provides a new interactive experience that can bring users into a virtual real world, providing a more realistic and immersive experience [4]. The application of virtual reality technology in the interactive interface design of public service advertisements can not only improve the user experience, but also allow users to have a deeper understanding of the information that public service advertisements are intended to convey [5]. In virtual reality technology, visual positioning is a very important technology, and more realistic positioning can improve the immersion and realism of virtual reality. Therefore, a study on the interactive interface design of public service advertising has proposed an interface design method that integrates virtual reality technology and visual positioning, in order to provide more reference solutions for the interactive interface design of public service advertising.

The research mainly focuses on four aspects. The first part discusses the current research achievements in interactive interface design and virtual reality technology. The second part elaborates on the technical methods used in the research and design of interactive interface design methods for public service advertisements that integrate virtual reality technology. The third part is to test the performance of the research method. The last part is a discussion and summary of the entire text.

## II. Related Works

Public service announcements (PSAs) are one of the most important tools for spreading healthy moral values in society, and the large number of PSAs being broadcast has led experts to realise the value of applying interactive interfaces to PSAs. A number of experts have conducted research on interactive interface design, and Zong J and others have proposed a system based on Lyra 2 to address the problem that interactive graphic interface design is limited to static output. The process uses a trial-and-error approach to define the attributes of interaction and then represent the interaction on the editorial visualisation. Experimental results show that the proposed method is effective in expressing interactions in multiple types of interface design and has a high runtime speed [6]. Oulasvirta A et al. propose a combinatorial optimisation approach to the problem of coding in the design of interactive GUIs. The process identifies the problem type, selects the focus of the design goals and formulates the functionality specifically. Experimental results show that the proposed approach has good human-computer interaction and can

effectively design interactive interfaces [7]. Latif S et al. propose a correlation method to support the tight coupling of data text and diagrams for the adoption of complex data for graphical text interfaces. The process developed a hybrid active interface to enable users to construct interactive interface references between the chart texts. The end result shows that the method is an effective way to provide a wide range of users with the ability to write interactive data documents [8]. Leung J and Cockburn A propose a structured design framework for improving the control and application performance of salient display techniques in user interface design, involving parameter control and highlighting constructs (PCCH). The process collected and reviewed a range of potential human factors and effect measures regarding the interactive impact of highlighting techniques. The results show that the framework is effective in improving the user's understanding of salient information[9]. Two scholars, Jianan L and Abas A, analyse human-computer interaction and the safety and comfort of car driving. The process provides an effective analysis of future human-machine interaction modes and proposes a method for designing human-machine interface interactions with cars based on existing technologies, providing some reference for future car human-machine interface design [10].

There have also been studies on virtual reality technology by experts. Qiu W et al. propose a parallel hierarchical control method based on virtual reality in order to be able to construct a large-scale high-fidelity traffic scene simulator. The process modifies and generates the original data of the traffic elements and assigns all the data to the corresponding taskers based on the proposed spatially parallel slicing method. The results show that the method can effectively ensure the fidelity of the visual scene and better allocate computational resources [11]. Hite R L et al. propose an effective combination of three-dimensional modelling (3D), support for haptic feedback (HE) and interactive virtual reality (VR) in order to assist all K-12 learners in their curriculum on human heart and physiology, and apply it to the curriculum. The results show that the application of 3D-HE-VR technology can effectively provide learners with powerful system representations and student-driven interactions, significantly driving system learning forward [12]. Gu K et al. propose a virtual reality-depth image based rendering (DIBR) method for effective assessment of the quality of synthetic images. To accomplish this goal, the study introduced a new blind image quality assessment (IQA) method developed through multi-scale natural scene statistical analysis (MNSS). The results show that the method has a more comprehensive performance [13]. Rockcastle S et al. designed an experiment for illumination perception in a real space using a series of illuminators in order to make valid observations of images in real and simulated spaces. The process invited 53 people to perform immersive perception. The results showed that there was little difference between the perceived ratings of the designed virtual reality scene and people in the real space in a well-lit scene, which had a more realistic effect [14]. Yeh H C et al. used virtual reality technology in order to enable students to better grasp the language content and language skills in English and to reform the curriculum with virtual reality, interactive, audio and structured teaching. The results showed that students were better able to learn cross-culturally with VR technology and significantly improved their own English language learning skills [15].

In summary, although virtual reality technology has been studied and applied in many fields, there is a lack of research in the field of interactive interface design for public service announcements. In view of this, the study proposes an interactive interface design method for public service announcements that incorporates virtual reality technology in order to effectively design interactive interfaces for public service announcements and provide more references for the interactive interface design industry.

## III. Research on the Interactive Interface Design Method of Public Service Advertisement Integrating Virtual Reality Technology

### A. Design of Visual Orientation Methods for Interactive Interfaces

Interaction design supports people to communicate and interact with tools and objects in their working lives. In the Internet+ environment, PSAs are increasingly focused on interacting with their audiences to enhance the interest and content richness of functional PSAs [16-17]. Virtual reality technology is widely used in interactive games and software, and can be effectively applied to the design of interactive interfaces for PSAs due to its immersive nature and the variety of ways in which it can be used [18-19]. The main reference elements for interactive design are shown in Fig. 1.

As shown in Fig. 1, there are six principles and four elements to be considered when designing interactions. The four elements are: the object is the target user of the interaction; the behaviour is the action of the user during the interaction; the function is the interaction module and scenario that can be provided to the user during the interaction; and the technology is the implementation of the interaction. The technology is the control system and information algorithm that realises the interaction. Public service announcements (PSAs) have certain characteristics that differentiate them from ordinary advertisements in terms of planning and filming because of their special meaning of existence. The characteristics of an interactive PSA are shown in Fig. 2.

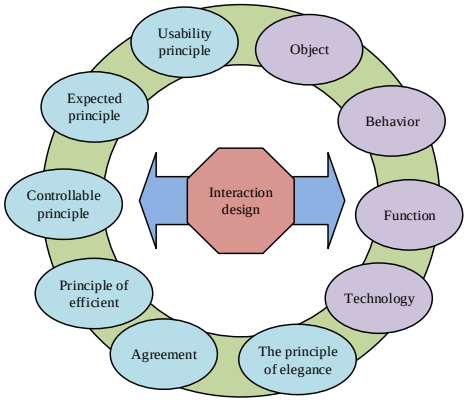


Fig. 1. Reference principles and elements of interaction design.

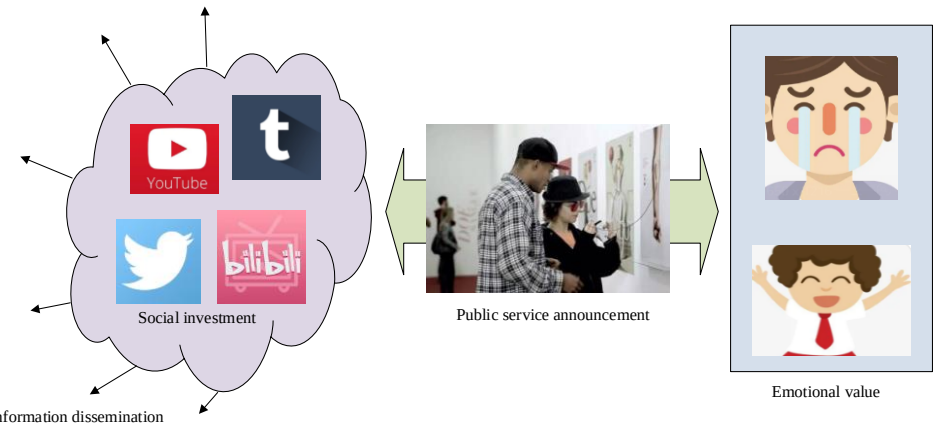


Fig. 2. Features of interactive public service announcement.

As can be seen from Fig. 2, interactive PSAs are a type of PSA, and so, like other PSAs, have two main characteristics: social input and emotional brewing. The development of the Internet has enabled information to spread faster and over a wider area, and social interaction has given rise to numerous information platforms through which the public can access public service information and play a supervisory role over social welfare. Public service announcements (PSAs) are more emotionally charged than ordinary advertisements, and interactive PSAs are richer in ways of communicating emotions, bringing a wider variety of emotional experiences to viewers as they interact with each other [20-21]. When designing interactive PSAs using virtual reality technology, the first step is visual positioning, analysing the information with location markers and solving for camera position and pose [22]. Before virtual reality can be used for spatial positioning, 2D markers need to be created. 2D markers are deformed in 3D space due to perspective, and 2D markers captured by the camera are more likely to be trapezoidal in shape, requiring a coordinate system conversion for recognition. In the pixel and image coordinate system, the dimensions of a single pixel on the u and v axes are shown in Eq. (1).

$$\begin{cases} u = x / d_x + u_0 \\ v = y / d_y + v_0 \end{cases} \tag{1}$$

In Eq. (1), $d_x$ represents the unit size of a single pixel on the x-axis; $d_y$ represents the size of a single pixel on the y-axis; $u_0$ and $v_0$ represent the coordinates of the centroids in the image coordinate system. The matrix relationship between pixels and images is shown in Eq. (2).

$$\begin{bmatrix} u \\ v \\ 1 \end{bmatrix} = \begin{bmatrix} 1/d_x & 0 & u_0 \\ 0 & 1/d_y & v_0 \\ 0 & 0 & 1 \end{bmatrix} \begin{bmatrix} x \\ y \\ 1 \end{bmatrix} \tag{2}$$

In Eq. (2), the matrix is normalised by $u$ and $v$. The relationship between a point in the world coordinate system and its position in the camera coordinate system is shown in Eq. (3).

$$P_c = RP_w + t \tag{3}$$

In equation (3), $P_c$ represents the coordinates of the point in the camera coordinate system; $P_w$ represents the coordinates of the point in the world coordinate system; and $R$ is the rotation matrix. After the rotation of the coordinate system by the rotation matrix, the relationship is matrixed and normalised to obtain the coordinate matrix, as shown in Eq. (4).

$$\begin{bmatrix} X_c \\ Y_c \\ Z_c \\ 1 \end{bmatrix} = \begin{bmatrix} r_{11} & r_{12} & r_{13} & t_x \\ r_{21} & r_{22} & r_{23} & t_y \\ r_{31} & r_{32} & r_{33} & t_z \\ 0 & 0 & 0 & 1 \end{bmatrix} \begin{bmatrix} X_w \\ Y_w \\ Z_w \\ 1 \end{bmatrix} \tag{4}$$

In Eq. (4), $X_c$, $Y_c$ and $Z_c$ represent the coordinates of the point in the three axes of the camera's coordinate system respectively; $X_w$, $Y_w$ and $Z_w$ represent the coordinates of the point in the three axes of the world coordinate system respectively. Since the camera lens uses a convex lens, there is bound to be aberrations when recording the image and the image needs to be corrected. With the centre of the aberration as the central point, the deviation along the radial direction is the radial aberration, and the radial aberration error is shown in Eq. (5).

$$\begin{cases} \varepsilon_{ur} = u(k_1 r^2 + k_2 r^4 + k_3 r^6) \\ \varepsilon_{vr} = v(k_1 r^2 + k_2 r^4 + k_3 r^6) \end{cases} \tag{5}$$

In Eq. (5), $\varepsilon_{ur}$ is the radial error of the point position on the u-axis of the pixel coordinate system; $\varepsilon_{vr}$ is the radial error of the point position on the v-axis of the pixel coordinate system; $k$ represents the radial aberration coefficient. The deviation along the tangent line with the centre of distortion as the centre point is the tangential distortion, and the tangential distortion error is shown in equation (6).

$$\begin{cases} \varepsilon_{tu} = 2p_1 uv + p_2(r^2 + 2u^2) \\ \varepsilon_{tv} = p_1(r^2 + 2v^2) + 2p_2 uv \end{cases} \tag{6}$$

In Eq. (6), $p$ represents the tangential aberration factor; $\varepsilon$ represents the aberration error of the coordinate axes. Thin lens aberrations occur when the camera lens is not parallel to

the CDD, and the thin lens aberration error is shown in Eq. (7).

$$\begin{cases} \varepsilon_{cu} = s_1(u^2 + v^2) \\ \varepsilon_{cv} = s_2(u^2 + v^2) \end{cases} \tag{7}$$

In Eq. (7), $s$ represents the thin lens aberration parameter.

### B. Design of an Interactive Interface Camera Positioning Method Based on Image Pre-processing

In the interactive interface of a PSA, the camera needs to extract the logo image for visual positioning, and using a higher resolution image can increase the accuracy of the extraction. However, the higher the resolution of the image, the more storage space it takes up and the greater the pressure on the system when processing the image [23]. The 2D logo used in the study is only in black and white, so the logo image can be extracted by greyscaling the image, which does not affect the visual localisation of the camera and reduces the amount of extra information contained in the image. The study uses the cvtColor greyscale function, which comes with the OpenCV vision library, to greyscale the images. The camera converts the image colour during imaging in the RGB domain, resulting in the appearance of non-linear noise[24]. The median filtering method takes care of bright and dark point noise and removes sharp signals from the signal. When performing telecoded image processing, reference points need to be extracted and the maximum contour containing all points is calculated as shown in Eq. (8).

$$\begin{bmatrix} (x_1, y_1) & \cdots & (x_1, y_n) \\ \vdots & \ddots & \vdots \\ (x_m, y_1) & \cdots & (x_m, y_n) \end{bmatrix} \in \max Quad\left((x_l, y_m), (x_n, y_o), (x_p, y_q), (x_r, y_w)\right) \tag{8}$$

In Eq. (8), $\max Quad$ represents the maximum contour that contains all points. As the operator interacts, the captured image will change due to the operator's actions and the study uses a perspective transformation to process the image. The principle of the perspective transformation is shown in Fig. 3.

As can be seen in Fig. 3, the captured image differs from the real one in shape in the final two-dimensional form because of the angle formed between the lens and the surface of the object and the perspective changes in the lens field of view, which are large near and far away. The coordinates of the original image and the pixel points of the transformed image are established, and the coordinates of the perspective transformed image are obtained after linear and translational transformations, as shown in Eq. (9).

$$\begin{cases} X^p = \dfrac{a_{11}X + a_{12}Y + a_{13}}{a_{31}X + a_{32}Y + a_{33}} \\ Y^p = \dfrac{a_{21}X + a_{22}Y + a_{23}}{a_{31}X + a_{32}Y + a_{33}} \end{cases} \tag{9}$$

In Eq. (9), $X^p$ and $Y^p$ represent the coordinates of the pixel points on the X and Y axes respectively. The Z-axis coordinates are both 1 after the transformation. In order to reduce the computational pressure of extraction, the 2D logo is rotated so that the logo is at a computationally convenient angle. The rotation angle of the logo is calculated as shown in Eq. (10).

$$angle = arc\left(\frac{y_2 - y_1}{x_2 - x_1}\right) \tag{10}$$

In Eq. (10), $angle$ represents the rotation angle; $x_1$ and $y_1$ are the centroid coordinates of the top left corner; $x_2$ and $y_2$ are the centroid coordinates of the top right corner. When locating near-code images, only the pixel coordinates of the image centroid need to be extracted. However, when searching for near-code image finding, the position image and the parent contour can interfere. The study uses an iterative method to mitigate the interference by establishing a hierarchical relationship for each contour and then removing the position image. This is shown in Fig. 4.

As seen in Fig. 4, the complete labelled image contour contains three position contours as well as the parent contour. The position contours are the first to be removed by the iteration as they differ most from the near-code image. The separate small squares in the near-code image are combined while the parent contours are removed, resulting in an image containing only the near-code image. The complete image pre-processing process is shown in Fig. 5.

As can be seen from Fig. 5, in the first half of the pre-processing process, the colour and interference noise of the image are processed, and the outline of the 2D logo is extracted and the area of the maximum outline is calculated. The maximum contour area is used as the judging condition, and the area requirement is met before entering the second half of the processing process for the far-code and near-code images, and when the maximum contour area exceeds the judging value, the image is judged as a near-code image, otherwise it is judged as a far-code image. After the extraction of information from the far code image or the near code image, the image pre-processing of the 2D logo is completed. The 3D reference point on the camera coordinate system is shown in Eq. (11).

$$P_i^c = RP_i^w + t \tag{11}$$

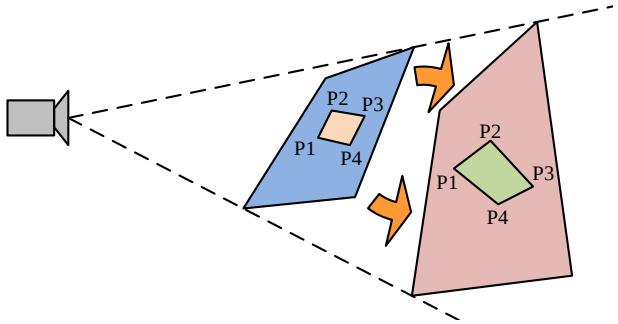


Fig. 3. Perspective schematic diagram.

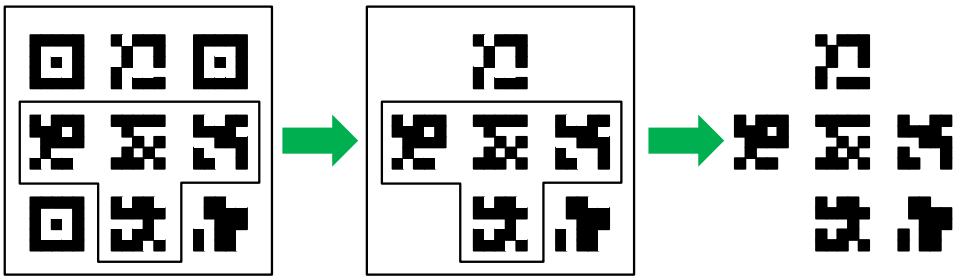

Fig. 4. Interference contour removal.

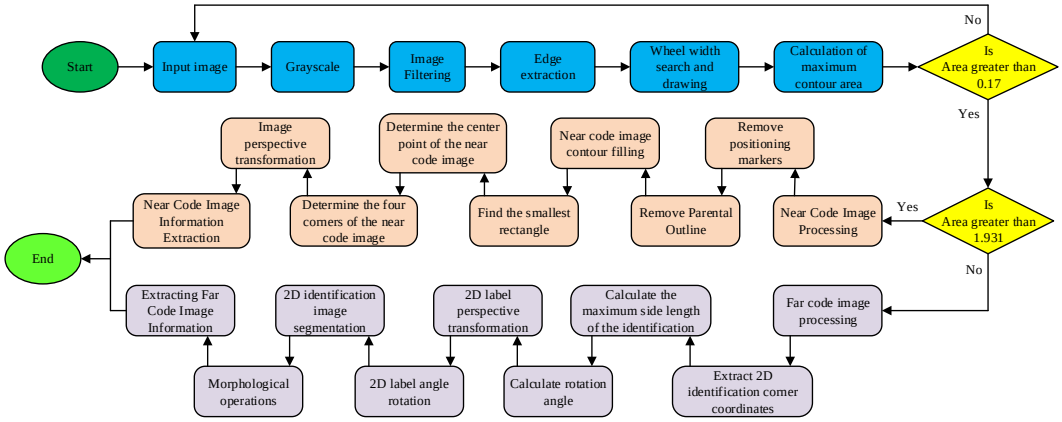


Fig. 5. 2D identification image preprocessing process.

In Eq. (11), $P_i^w$ represents the coordinates of the 3D reference point on the world coordinate system; $R$ is the rotation matrix obtained after the reference point enters the camera coordinate system; $t$ is the translation of the reference point after it enters the camera coordinate system. The reference point is subject to some error in actual positioning, and the study iterates over the object-squared residuals to complete the estimation of the camera's position pose. The object-squared residuals are calculated as shown in Eq. (12).

$$E_g = \left\| \dot{p}_i - \dot{p}_i^{'} \right\| = \left\| p_i - \frac{R(P_i^c - C)}{R^3(P_i^c - C)} \right\| = \frac{1}{Z_i^c} \left\| P_i^c - P_i^{'c} \right\| \tag{12}$$

In Eq. (12), $P_i^{'}$ and $P_i^{'c}$ are the reference estimation points; $\dot{p}_i$ represents the flush coordinates of the image reference point; $\dot{p}_i^{'}$ represents the flush coordinates of the estimation point; $C$ represents the coordinates of the origin on the world coordinate system; and $Z_i^c$ represents the depth value of the reference point on the camera coordinate system. The object-squared residuals and image-squared residuals are shown in Fig. 6.

As seen in Fig. 6, the depth of the spatial reference point affects the object residuals when the image residuals are the same, the deeper the object residuals the greater the object residuals. When performing the orthogonal iteration, the error between the theoretical point and the reference point in the 2D plane is calculated as shown in Eq. (13).

$$w_{ki} = \frac{1}{n} \sum_{i=1}^{n} \left( \frac{(u_i - \bar{u}_i)^2}{\bar{u}_i - u_0} \right) \tag{13}$$

In Eq. (13), $u$ represents the coordinates of the point after the distortion effect. The translation vector and rotation matrix are calculated by introducing the Kronecker product for matrix operations, as shown in Eq. (14).

$$\begin{cases} A \otimes (B + C) = A \otimes B + A \otimes C \\ (A \otimes E_1)(E_2 \otimes B) = A \otimes B \\ vec(ABC) = (C^T \otimes A) vec(B) \\ P_i^W \leftarrow P_i^W - \bar{P}_i^w \end{cases} \tag{14}$$

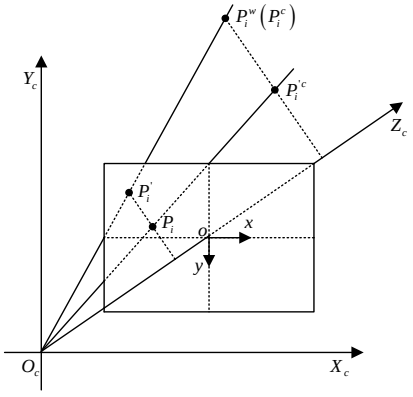


Fig. 6. Object residual and image residual.

In Eq. (14), $\bar{P}_i^w$ is the average of all spatial reference points. Decompose the matrix $m$ as shown in Eq. (15).

$$\begin{cases} m^{(k)} = \left[ \sum_{i=1}^{n} w_i \left( P_i^w \otimes \left( P_i^w \right)^T \otimes V_i^{'} \right) + \sum_{i=1}^{n} \left( P_i^w \otimes V_i^{'} \right) (G) \right] H^{(k)} \\ m = UDV^T \end{cases} \tag{15}$$

In Eq. (15), $m^{(k)}$ and $vec\left(M^{(k)}\right)$ are equal and are obtained by regularising the projection points. After calculating the translation vector and combining it with the rotation matrix, the objective function is obtained, as shown in Eq. (16).

$$\begin{cases} E(R,t) = \sum_{i=1}^{n} w_i \left\| \left( T - V_i^{'} \right) \left( \left( P_i^w \right)^T \otimes I + G \right) H \right\|^2 = H^T J_{9\times 9} H \\ J = \sum_{i=1}^{n} w_i \left( \left( P_i^w \right)^T \otimes I + G^T \right) \left( I - V_i^{'} \right) \left( \left( P_i^w \right)^T \otimes I + G \right) \end{cases} \tag{16}$$

In Eq. (16), the matrix at $G$ is considered a constant matrix; $E(R,t)$ represents the final camera position. Once the technical framework has been constructed, the design of the appearance and interactive functionality of the interactive PSA interface can be carried out.

## IV. Performance Testing of an Interactive Interface Design Method for Public Service Announcements Incorporating Virtual Reality Technology

In order to verify the feasibility and effectiveness of the research design virtual reality technology when applied to the design of interactive interfaces for public service announcements, the performance of the system was tested. The basic hardware environment setup for the experiment is shown in Table I.

The testing started with performance testing of the functions in the first half of the process. The performance of the study using the greyscale algorithm was tested and compared with other greyscale algorithms and the results are shown in Fig. 7.

As can be seen in Fig. 7(a), the smallest result in the peak signal-to-noise ratio test was obtained by the component method at 12.980dB, while the largest result was obtained by the cvtColor used in the research method at 13.390dB. 39.053; the study method is not the largest, but the value of 39.021 is very close to the maximum. This shows that the research method produces the clearest images, with higher image contrast and higher computational efficiency. The performance of the denoising algorithm was tested and compared with other denoising algorithms and the results are shown in Fig. 8.

As seen in Fig. 8(a), the test was conducted using lightly shaded images, moderately shaded images, and heavily shaded images. In the signal-to-noise ratio test, the median filter reaches a value of 35.635dB on the light shaded image, much higher than the Gaussian filter and the mean filter at 28.595dB and 28.526dB; the median filter is the same as the mean filter on the medium shaded image, both at 25.673dB, slightly lower than the Gaussian filter at 25.841dB, but the difference is negligible; the median filter reaches a value of 38.145dB on the heavy shaded image, much higher than the Gaussian filter and the mean filter. As can be seen from Fig. 8(b), the mean square error of the median filter on the light, medium and heavy shaded images is lower than 14, and the lowest mean square error of the Gaussian filter and the mean filter is 24.666, which is much higher than that of the median filter. This indicates that the research method can provide good denoising of images in light, medium and heavy shading environments. After completing the testing of the first half of the process function, the performance of the research method was tested. The noise was fixed at 3pixel and 1000 experiments were performed for each reference point. The error of the research method when the number of reference points was varied was tested and the results are shown in Fig. 9.

TABLE I. The Experiment's Basic Environmental Parameters

| Parameter variables | Parameter selection |
|---|---|
| Operating system | Windows 10 |
| Operating environment | MATLAb 2020a |
| System PC side memory | 16G |
| CPU dominant frequency | 2.62Hz |
| GPU | RTX-2060 |
| Central Processing Unit | Intel ⑧CoreTM i5-10500 |

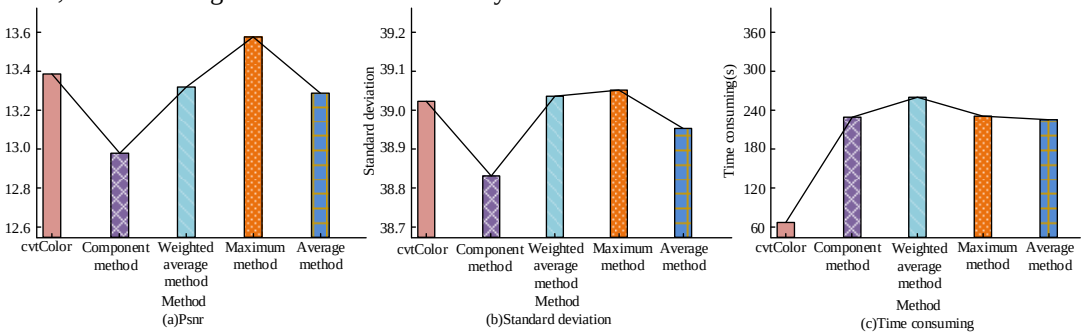


Fig. 7. Comparison of grayscale algorithm performance.

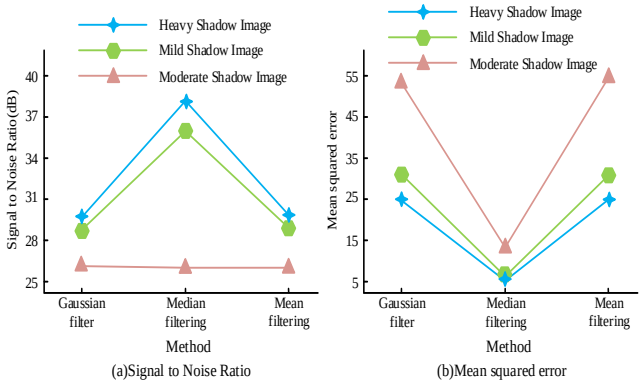


Fig. 8. Noise reduction effect test.

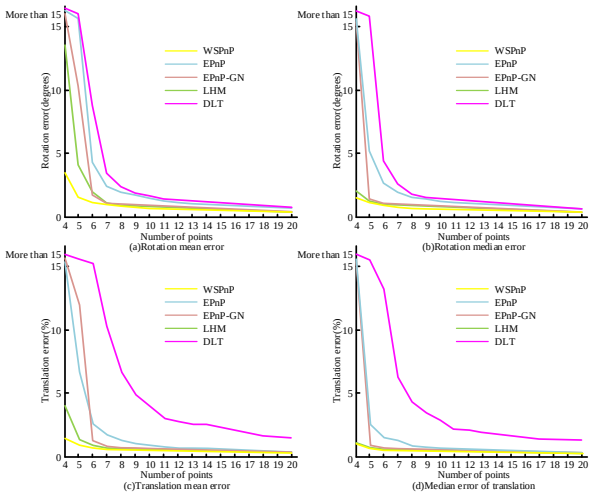


Fig. 9. Rotation error and translation error.

As can be seen from Fig. 9, the errors of all methods gradually decrease as the number of reference points increases. As seen in Fig. 9(a) and Fig. 9(b), the curves for all methods show a sharp decrease in the first few times and a slow decrease towards a stable shape in the later stages in terms of rotational mean error and rotational median error. The rotational mean error of the study method at 4 reference points is about 4.2degrees, much lower than the other methods, and the rotational median error at four reference points is about 2.1degrees, slightly lower than the LHM and much lower than the other remaining methods. At reaching 20 reference points, the rotational mean error of the study method stabilises around 0.7degrees, slightly lower than the other methods; the rotational median error of the study method stabilises around 0.6degrees, slightly lower than the other methods. As can be seen from Fig. 9(c) and Fig. 9(d), the curves of all the methods show a sharp decline in the first few times and a slow decline towards stability in the latter part of the curve for both the translational mean error and the translational median error, with the DLT declining at a slightly slower rate. The mean error of translation at 4 reference points is slightly lower than the LHM and much lower than the remaining methods, while the median error of evaluation is slightly lower than the LHM and much lower than the remaining methods. When reaching 20 reference points, the translation mean error of the study method and all other methods except DLT are stable at around 0.5%, and the translation median error is stable at around 0.4%. This indicates that the error of the research method is less affected by the number of reference points and has a much lower error. The effect of Gaussian noise on the positioning accuracy was tested and is shown in Fig. 10.

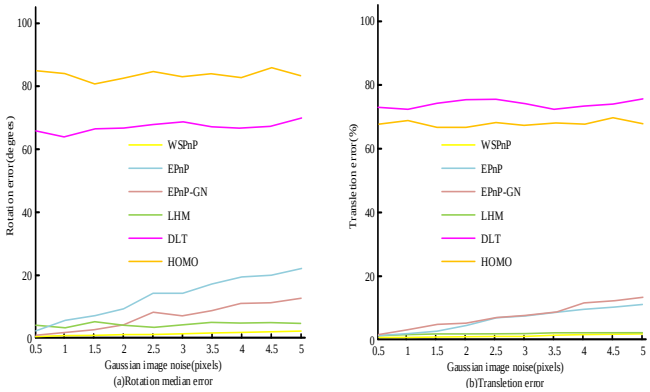


Fig. 10. The influence of Gaussian noise on location accuracy.

As can be seen in Fig. 10, DLT and HOMO consistently remain at a high error level when performing localisation, with the other methods resulting in increasing errors as the Gaussian noise increases. In terms of rotation error, the rotation error of the study method is about 0.3degrees at 0.5pixels, rising to about 1.8degrees when reaching 5pixels, which is significantly lower than the other methods. In terms of translation error, the translation error of the research method is about 0.1% at 0.5pixels and rises to about 1.2% at 5pixels, which is closer to LHM and significantly lower than other methods. This indicates that the de-noising performance of the research method is good, and the performance advantage of the research method becomes more obvious when the Gaussian noise is larger. Ten 3D reference points were set, and the camera coordinates for the 3D reference points were solved and reprojected, as shown in Fig. 11.

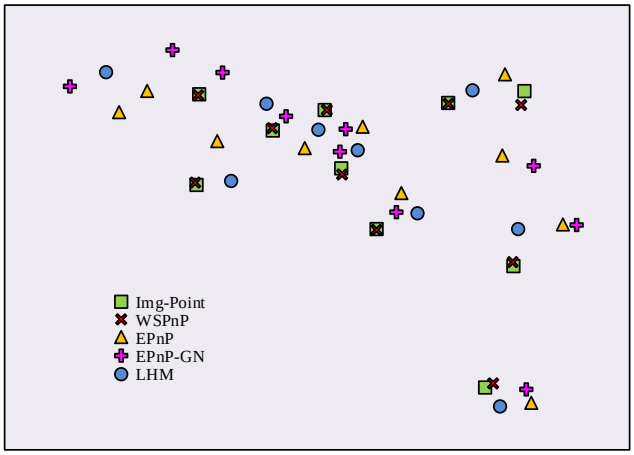


Fig. 11. Image plane reprojection.

As can be seen from Fig. 11, the 10 original image points are randomly distributed in the image plane, the reprojection position of EPnP-GN deviates more, only 6 points are closer to the original image points; EPnP and LHM have more points

closer to the original image points, but no points almost coincide with the original points. All the points of the research method are close to the original points, and seven of them almost coincide with the original points. This indicates that the research method has good performance in solving the coordinates and produces less variation in position. The research method was tested with different numbers of reference points, as shown in Fig. 12, to ensure the computation time and number of solutions when using the research method for PSA interactive interface design.

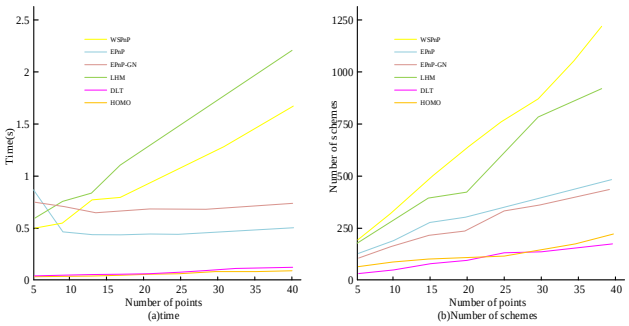


Fig. 12. Calculation time and number of generated solutions.

The computation time of EPnP-GN and EPnP does not depend much on the number of reference points, while the computation time of other methods including the research method increases with the number of reference points. The computation time of EPnP-GN and EPnP is basically stable at 0.6s and 0.8s. DLT and HOMO are linear solution methods with obvious advantages in speed, but lacking in accuracy. The computation time of the research method is about 0.5s at five reference points, rising to about 1.6s when 40 reference points are reached, more than EPnP-GN and EPnP when the number of reference points is higher, and in all cases lower than LHM, which also uses orthogonal iteration. The research method generates 212 solutions at five reference points and rises to 1203 solutions at 40 reference points, which is more than the other algorithms. This indicates that the research method does not have a significant speed advantage when designing interactive interfaces for PSAs, but it can generate more solutions and provide a richer choice when conducting subsequent designs.

## V. Conclusion

The interactive interface design of public service advertising directly affects the quality of public service advertising. In the environment of virtual reality technology, the visual positioning method is designed first, and then when the camera positioning method is designed, the image is preprocessed to reduce the computational burden, the Iterative method is introduced to reduce the interference in image positioning, and finally the object residual is iterated to complete the camera position pose estimation. The results show that the research method only requires 65.804ms for image graying, while other methods require over 200ms; The Mean squared error of research methods on light, medium and heavy shadow images is lower than 14, far lower than other methods; In a noisy environment of three pixels, the translation mean error of the research method is around 0.5%, and the translation median error is around 0.4%, which is lower than other methods; In the Gaussian noise environment of five pixels, the rotation error of the research method is 1.8 degrees, which is significantly lower than other methods; When designing research methods, using five reference points can generate 212 schemes, which is more than other methods. It shows that the research method has good technical performance guarantee under the virtual reality technology environment, and can provide more options for the design of other content such as the Look and feel of subsequent public service advertisements. However, the research was tested in a simulated environment and lacked data reference to the real environment. In the future, real machine testing will be conducted to enrich experimental data and optimize it.

## References

[1] Oulasvirta A, Dayama N R, Shiripour M, John M, Karrenbauer A. Combinatorial Optimization of Graphical User Interface Designs. Proceedings of the IEEE, 2020, 108(3):434-464.

[2] Chen M, Fadel G, Mata I. Applications of affordance and cognitive ergonomics in virtual design: A digital camera as an illustrative case:. Concurrent Engineering, 2022, 30(1):5-20.

[3] Yan X, Raj S, Huang B, Sun Y P, Newman M W. Toward Lightweight In-situ Self-reporting: An Exploratory Study of Alternative Smartwatch Interface Proceedings of the ACM on Interactive Mobile Wearable and Ubiquitous Technologies, 2020, 4(4):1-22.

[4] Kwok A, Yan M, Deng X H, Chen X Y, Huang Y T. Exploring the facilitating and obstructing factors of using virtual reality for 5S training: an exploratory qualitative study from students' perspectives in an industrial engineering undergraduate course. computer applications in engineering education. 2022, 30(4):1072-1085.

[5] Vergel R S, Tena P M, Yrurzum S C, Cruz-Neira C. A Comparative Evaluation of a Virtual Reality Table and a HoloLens-Based Augmented Reality System for IEEE Transactions on Human-Machine Systems, 2020, 50(4): 337-348.

[6] Zong J, Barnwal D, Neogy R, Satyanarayan A. Lyra 2: Designing interactive visualizations by demonstration. IEEE Transactions on Visualization and Computer Graphics, 2020, 27(2): 304-314.

[7] Oulasvirta A, Dayama N R, Shiripour M, John M, Karrenbauer A. Combinatorial optimization of graphical user interface designs. Proceedings of the IEEE, 2020, 108(3): 434-464.

[8] Latif S, Zhou Z, Kim Y, Beck F, Kim N W. Kori: Interactive synthesis of text and charts in data documents. IEEE Transactions on Visualization and Computer Graphics, 2021, 28(1): 184-194.

[9] Leung J, Cockburn A. Design framework for interactive highlighting techniques. Foundations and Trends® in Human-Computer Interaction, 2021, 14(2-3): 96-271.

[10] Jianan L, Abas A. Development of Human-Computer Interactive Interface for Intelligent Automotive. international Journal of Artificial Intelligence, 2020, 7(2):13-21.

[11] Qiu W, Shangguan W, Chai L, Cai B, Chen J J. Parallel Hierarchical Control-based Efficiency Enhancement for Large-scale Virtual Reality Traffic Simulation. IEEE Intelligent Transportation Systems Magazine, 2021, 14(4): 145-162.

[12] Hite R L, Jones M G, Childers G M, Ennes M E, Chesnutt K M, Pereyra M, Cayton E M. The utility of 3D, haptic-enabled, virtual reality technologies for student knowledge gains in the complex biological system of the human heart. journal of computer assisted learning, 2022, 38(3):651-667.

[13] Gu K, Qiao J, Lee S, Liu H, Lin W, Callet P L. Multiscale Natural Scene Statistical Analysis for No-Reference Quality Evaluation of DIBR-Synthesized Views. IEEE Transactions on Broadcasting, 2020, 66(1):127-139.

[14] Rockcastle S, Danell M, Calabrese E, Sollom-Brotherton G, Mahic A, Wymelenberg K. Comparing perceptions of a dimmable LED lighting system between a real space and a virtual reality display:. Lighting Research & Technology, 2021, 53(8):701-725.

[15] Yeh H C, Tseng S S, Heng L. Enhancing EFL students' intracultural learning through virtual reality. interactive Learning Environments, 2022, 30(9): 1609-1618. Environments, 2022, 30(9): 1609-1618.

[16] Alsswey A H, Al-Samarraie H, El-Qirem F A, Alzahrani A I, Alfarraj O. Culture in the design of mHealth UI: An effort to increase acceptance among The Electronic Library, 2020, 38(2):257-272.

[17] Ahmed S K, Naji Z H, Hatif Y N, Hussam M. Design and Implementation of a Computerized Drug Inventory Management Information System Using ASP.NET MVC. Diyala Journal of Engineering Sciences, 2020, 13(4):80-90.

[18] Yang Y, Song X. Research on face intelligent perception technology integrating deep learning under different illumination intensities. journal of Computational and Cognitive Engineering, 2022, 1(1): 32-36.

[19] Lei Y. Research on microvideo character perception and recognition based on target detection technology. journal of Computational and Cognitive Engineering, 2022, 1(2): 83-87.

[20] Savickaite S, Mcnaughton K, Gaillard E, Amaya J, Mcdonnell N, Millington E, Simmons D R. Exploratory study on the use of HMD virtual reality to investigate individual differences in visual processing styles. journal of enabling technologies. 2022, 16(1): 48-69.

[21] Amin S N, Shivakumara P, Jun T X, Chong K Y, Zan D L L, Rahavendra R. An Augmented Reality-Based Approach for Designing Interactive Food Menu of Restaurants Using Android//Artificial Intelligence and Applications. 2023, 1(1): 26-34.

[22] Ugur E, Konukseven B O. The potential use of virtual reality in vestibular rehabilitation of motion sickness. auris, nasus, larynx, 2022, 49(5):768 -781.

[23] Islam A, Othman F, Sakib N, Babu H M H. Prevention of Shoulder-Surfing Attack Using Shifting Condition with the Digraph Substitution Rules//. Artificial Intelligence and Applications. 2023, 1(1): 58-68.

[24] Vergara D, Anton-Sancho A, Davila L P, Fernandez-Arias P. Virtual reality as a didactic resource from the perspective of engineering teachers. Computer applications in engineering education, 2022, 30(4):1086-1101.